

CRUSTAL STRUCTURE OF THE SOUTHERN CALAVERAS FAULT ZONE, CENTRAL CALIFORNIA, FROM SEISMIC REFRACTION INVESTIGATIONS

BY PETER BLÜMLING*, WALTER D. MOONEY, AND W. H. K. LEE

ABSTRACT

A magnitude 5.7 earthquake on 6 August 1979, within the Calaveras fault zone, near Coyote Lake of west-central California, motivated a seismic-refraction investigation in this area. A northwest-southeast profile along the fault, as well as two fan profiles across the fault were recorded to examine the velocity structure of this region.

The analysis of the data reveals a complicated upper crustal velocity structure with strong lateral variations in all directions. The near-surface layers consist of recent sediments with seismic *P*-wave velocities of 2.6 to 3.2 km/sec. These are underlain by rocks of the Great Valley Sequence which have an average velocity of 4.5 km/sec. The Great Valley Sequence is present along the whole profile; depths range from 4.3 to 4.8 km in the northwest near Anderson Lake and in the southeast of the profile line near Hollister. In the middle of the profile near Coyote Lake, however, this layer thins and we find a laterally limited higher velocity layer (5.1 km/sec) between depths of 2.8 to 4.8 km. The high-velocity zone, which coincides with a gravity high, also correlates spatially with the hypocentral area of the 6 August earthquake and its aftershocks and may therefore represent an asperity on the fault.

Velocities within the fault zone were determined from the fan profiles. Near Anderson Lake, a pronounced delay of first arrivals on the fan records indicates a vertical 1- to 2-km-wide near-surface, low-velocity zone along the fault. Near Coyote Lake, the delays observed in the fan records correlate with two subsurface en-echelon fault planes which have been previously identified from lineations in the seismicity pattern.

The structure of the lower crust is similar to the neighboring Diablo Range: a 8- to 9-km-thick upper crustal layer with a seismic velocity of 5.7 to 6.3 km/sec is underlain by a 3-km-thick layer with velocity 6.8 km/sec. In accordance with previous studies of the Diablo Range, there are indications of a pronounced lower crustal low-velocity zone between a depth of 17 and 23 km. The presence of this low-velocity zone suggests that higher velocity (igneous?) rocks of the middle crust have been thrust over sedimentary rocks.

INTRODUCTION

On 6 August 1979, a magnitude 5.7 earthquake occurred along the Calaveras fault zone in the Coyote Lake area of central California. This earthquake and its aftershocks took place within a very dense seismic network. However, the rms residuals for *P*-wave arrivals at many of the network stations were as high as 0.25 sec due to the laterally heterogeneous structure of this area which deviates from the regional one-dimensional velocity model routinely used to determine earthquake locations (Lee *et al.*, 1979).

In 1981, the U.S. Geological Survey conducted a seismic-refraction profile along the Calaveras fault in the Coyote Lake area to obtain *P*-wave velocity information within and near the fault zone. In this paper, we interpret these explosion-seismic

* Permanent address: Geophysikalisches Institut, Universität Karlsruhe, Karlsruhe-West, West Germany.

data and provide a detailed model of the upper crustal structure. When combined with the results of other crustal structure studies in the nearby Diablo Range (Walter and Mooney, 1982; Blümling and Prodehl, 1983), the Santa Clara Valley, and the Santa Cruz Mountains (Mooney and Luetgert, 1982), this investigation allows us to assess the degree of lateral variation in crustal structure in this area.

GEOLOGICAL SETTING

The Calaveras fault, part of the San Andreas fault system, is one of the most seismically active faults in central California. This fault and its southern continuation, the Paicines fault, are part of right-slip fault zones that branch northeastward from the San Andreas fault south of Hollister (Figure 1). The Calaveras-Paicines fault zone is more than 170 km in length, extending northward through Hollister

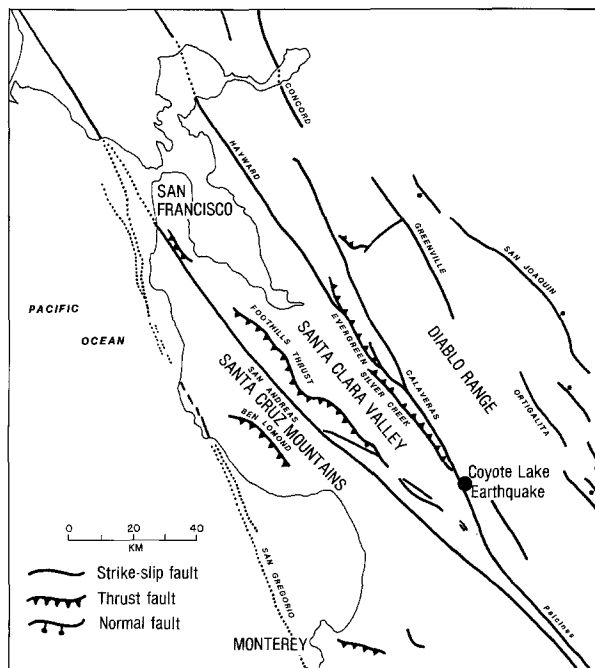


FIG. 1. Principal active faults of central California; study area (Figure 2) is the region along the Calaveras fault near the epicenter of the Coyote Lake earthquake. Generalized from Herd and McCulloch, 1983.

to Suisan Bay. Just east of San Jose the Hayward fault zone splays westward from the Calaveras. The tectonic movement in the San Francisco Bay region is complex and has been discussed by Herd (1979) and Page (1982a). It involves at least right-lateral strike-slip motion along the San Andreas, Calaveras, and Hayward faults, thrusting along the Foothills, Silver Creek, and Ben Lomand faults. Page (1982b) presents a modern review of the Calaveras fault zone, and Bakun (1980) summarizes the seismic activity on its southern reach for a 10-yr period beginning in 1969.

In the epicentral area of the Coyote Lake earthquake (Figure 2), the Calaveras fault zone borders the west side of the Diablo Range. The fault runs within low foothills on the east side of the Santa Clara Valley. The fault zone is a northwest-trending trench in which Coyote Lake and Anderson Lake are impounded. Eastward-dipping Great Valley sequence sandstones, shales, and conglomerates of

Cretaceous age east of the Calaveras fault zone are juxtaposed against small bodies of serpentine, Jurassic-Cretaceous Franciscan assemblage shale, Tertiary volcanics, and Pliocene and Pleistocene sedimentary rocks (Figure 2). North of Hollister, the Calaveras fault crosses the southern end of the Santa Clara Valley, offsetting both late Pleistocene and Holocene alluvium. The fault zone is vertical to nearly vertical in practically all exposures.

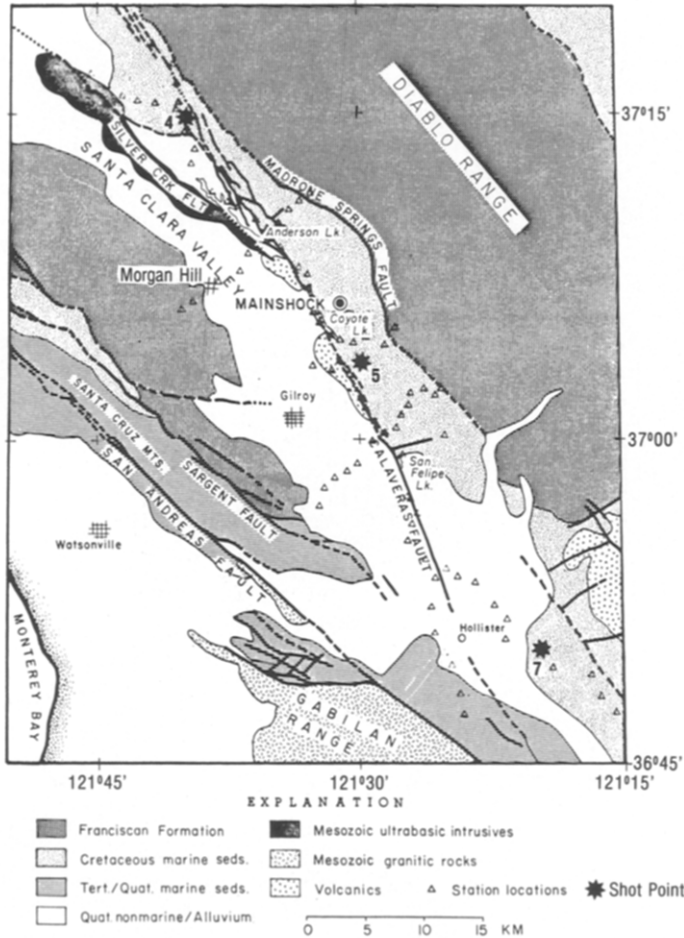


FIG. 2. Simplified geological map of the Calaveras fault region showing locations of the shotpoints, the seismograph stations, and the epicenter of the Coyote Lake main shock.

SEISMIC-REFRACTION DATA

The seismic-refraction survey conducted along the Calaveras fault consisted of a main reversed profile with an average station spacing of 1 to 2 km and two fans perpendicular to the main line. The experiment was designed to determine velocities within and near the fault zone from the reversed profile, and to quantify lateral velocity changes from the fan profiles. The main profile is about 70 km long and parallels the NW-SE trend of the fault zone. The fan profiles cross the fault zone near the towns of Morgan Hill and Gilroy (Figure 2). A total of 100 stations recorded arrivals from three shotpoints that are numbered as 4, 5, and 7.

Shot point 7 was situated in Cretaceous marine sediments near the southern edge of the Santa Clara Valley, and for logistical reasons this shotpoint could not be placed directly in the fault zone (i.e., in downtown Hollister). The other shotpoints were located directly within the fault zone: shotpoint 5 near Coyote Lake and shotpoint 4 north of Anderson Lake (Figure 2). The spacing between the shotpoint was approximately 26 km. The shots consisted of 800 kg of ammonium nitrate fired in 40-m-deep drill holes.

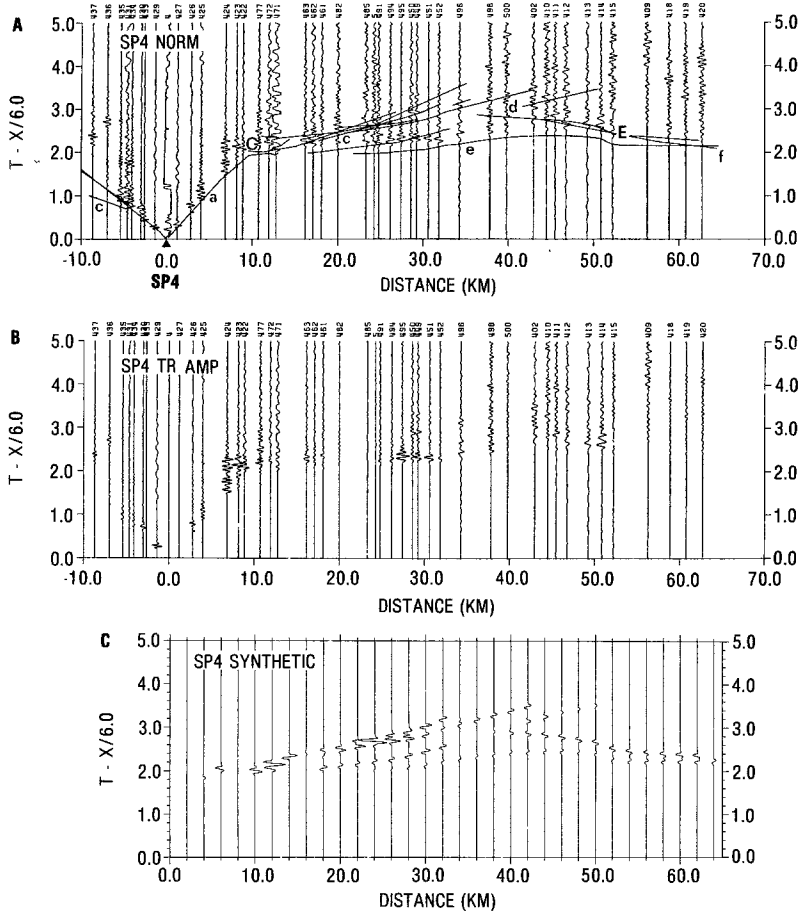


FIG. 3. Normalized and true-amplitude record sections (reduction velocity 6.0 km/sec) for shotpoint 4 in the southeast direction. The travel times (solid lines in A) are calculated for the velocity model of Figure 7. The synthetic seismograms, C, are plotted below the true-amplitude section, (B) Labels used for the various phases are explained in Figure 6.

THE MAIN PROFILE

The seismograms of the main profile were plotted as record sections with a reduction velocity of 6.0 km/sec (Figures 3 to 5). These sections provide the basis of our investigation. The interpretation procedure used was forward modeling utilizing a ray tracing program (Červený *et al.*, 1977) in order to fit the travel times for the first and secondary arrivals of the seismograms. In addition, synthetic seismograms were determined using the method of McMechan and Mooney (1980). These synthetic seismograms provided a guide for refining the velocity structure. The refracted and reflected phases observed on the record sections are identified as described in Figure 6.

The seismic data indicate some variations in the velocity of the upper layer. The record sections observed from shotpoint 4 (Figure 3) and shotpoint 7 (Figure 4) indicate near-surface *P*-wave velocities of 2.6 km/sec in the northwest and 2.7 to

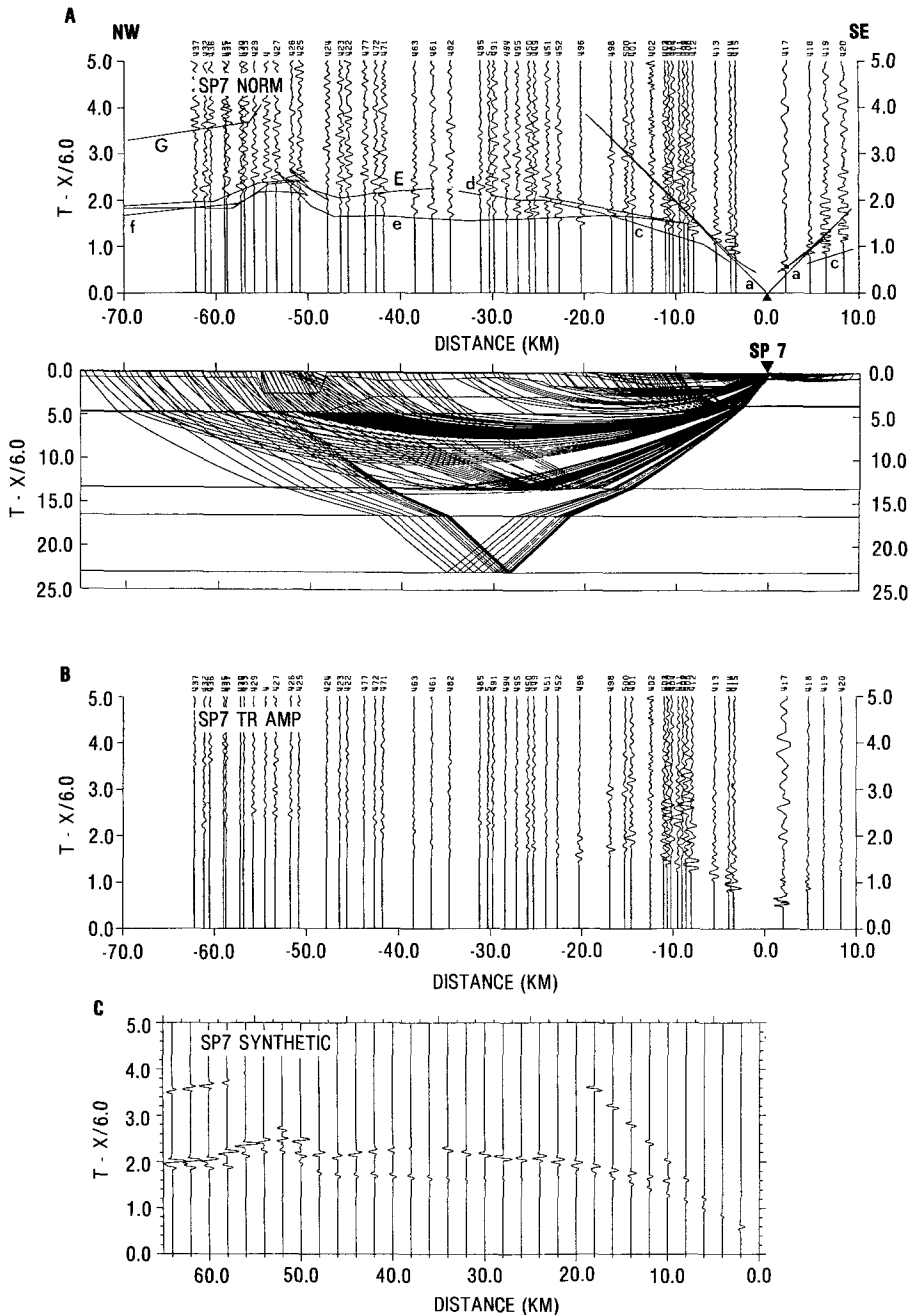


FIG. 4. Normalized and true-amplitude record sections for shotpoint 7 in the northwest direction. Presentation as for Figure 3, but with the ray trace diagram below the normalized record section.

2.8 km/sec in the southeast (Figure 7). In the middle of the profile, a somewhat higher velocity of 3.0 km/sec is observed for the near-surface layer. The thickness of the layer is quite variable; to explain delayed arrivals from deeper horizons it was

necessary to introduce a sedimentary basin near shotpoint 4 that is about 7 km long and 2.5 km deep (Figure 7). The arrival time delays are best illustrated by phase *e*, a refraction from a layer with a velocity of 5.7 km/sec at its top and 6.3 km/sec at

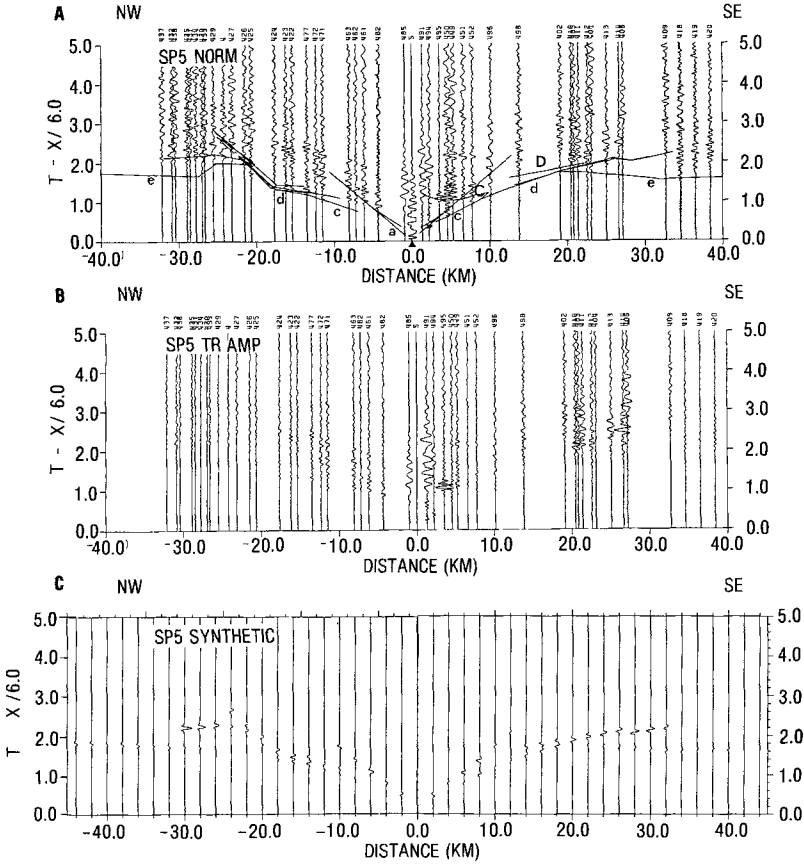


FIG. 5. Normalized and true amplitude record sections for shotpoint 5 to the northwest and southeast. Presentation as in Figure 3.

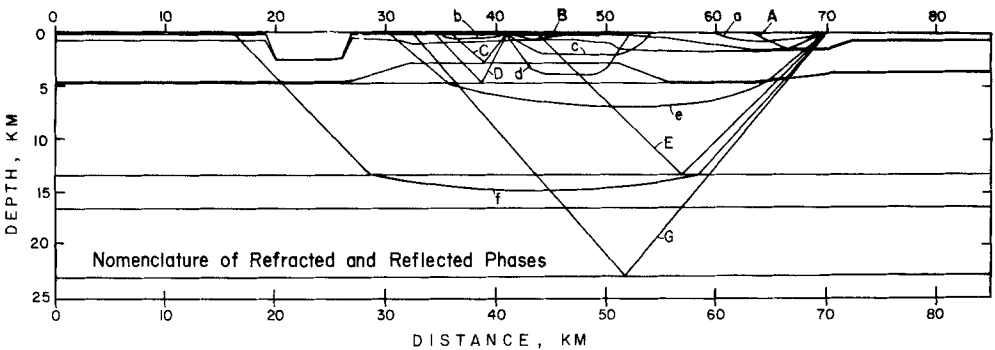


FIG. 6. Explanation of the labels used to identify the different seismic phases. Refracted phases are labeled with letters a to f, while the corresponding reflected phases are labeled with capital letters.

its bottom, that has a relative delay of more than 0.5 sec in the record section of shotpoint 4 (Figure 3). Further information on this small sedimentary basin is given by the record section of shotpoint 7 (Figure 4). In the range of -50 to -60 km

(negative distance indicates rays propagating to the northwest) from shotpoint 7 there is a clear travel-time delay of both the first arrivals (phase *e*) and the secondary arrivals (phase *f*), corresponding to the area of the sedimentary basin.

South of the basin, near Coyote Lake (near shotpoint 5, Figure 7), the sedimentary cover is less than 1 km thick, but increases continuously from shotpoint 5 in a southeasterly direction to a maximum thickness of 2 km in the southern Santa Clara Valley (at 55 km on Figure 7).

The next deepest layer has an average velocity close to 4.5 km/sec. The rays refracted within this layer are indicated by the letter *c* and the corresponding reflected waves from the bottom are labeled *C*. Refractions from this layer can be correlated as first arrivals in the record section of shotpoints 5 and 7, and as secondary arrivals in the record section of shotpoint 4. Because of the variations in

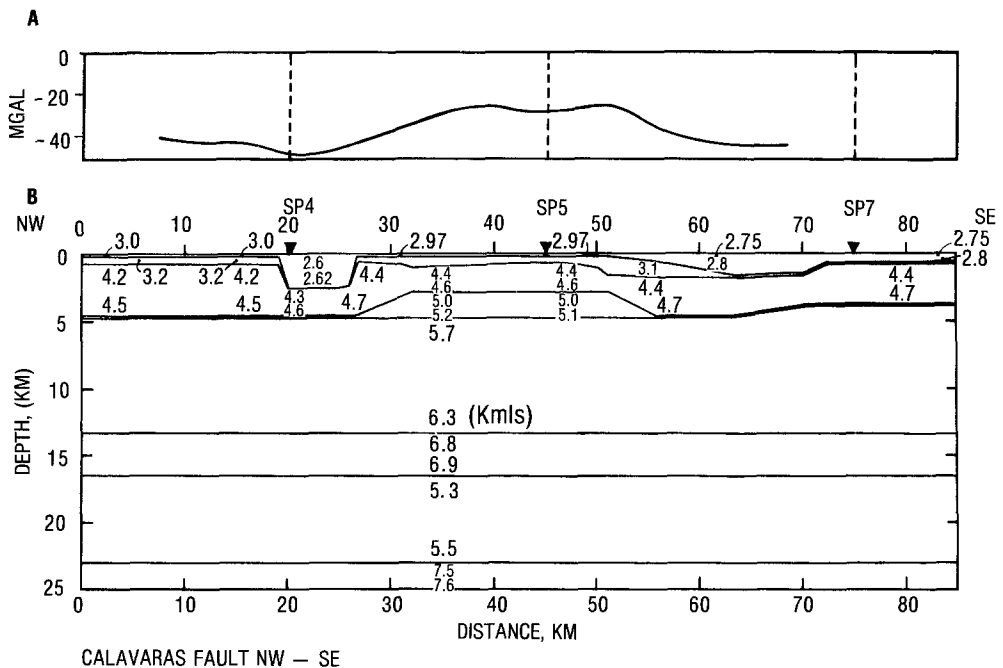


FIG. 7. Velocity-depth model (B) derived for the Calaveras fault region. The respective velocities kilometers/second are assigned above and below the layer boundaries. The positions of the shotpoints are shown by the triangles. The correspondence between the near-surface velocity structure and the Bouguer gravity anomaly along the profile (A) is evident.

thickness of the near-surface layer, and in particular because of the vertical boundaries of the sedimentary basin, phase *c* splits into several branches. This is illustrated by the synthetic record section shown in Figure 5. In the distance range where this splitting of rays occurs (-21 to -26 km), we could not accurately calculate synthetic seismograms, because the algorithm is based on ray tubes defined by successive rays (McMechan and Mooney, 1980). The lower boundary of the 4.5 km/sec layer varies in depth from 4.3 km near shotpoint 7 to 2.8 km near shotpoint 5, with significant variations in between. Northwest of shotpoint 5, the boundary remains at a nearly constant depth until 30 km range where it increases again to 4.8 km depth (Figure 7).

Phase *d* observed from shotpoint 5 (Figure 5) requires a layer with a velocity of about 5.1 km/sec. This phase appears as a first arrival in both the southeast and

the northwest portions of the refraction profile. However, it is not observed in the record sections of shotpoints 4 or 7, thus indicating that the layer is of limited dimensions (Figure 7).

The subsequent layer has a velocity from 5.7 to 6.3 km/sec and a constant thickness of 8 km. Refractions from this layer (phase *e*) form first arrivals between about 20 and 65 km. This layer correlates well in depth, thickness, and velocity with a layer interpreted in the Diablo Range to the east (Walter and Mooney, 1982; their Figure 2).

The structure of the deeper crust could only partially be determined because the maximum recording distance was only 65 km. Phases refracted and reflected within the lower crust are evident as secondary arrivals in the record sections of shotpoints

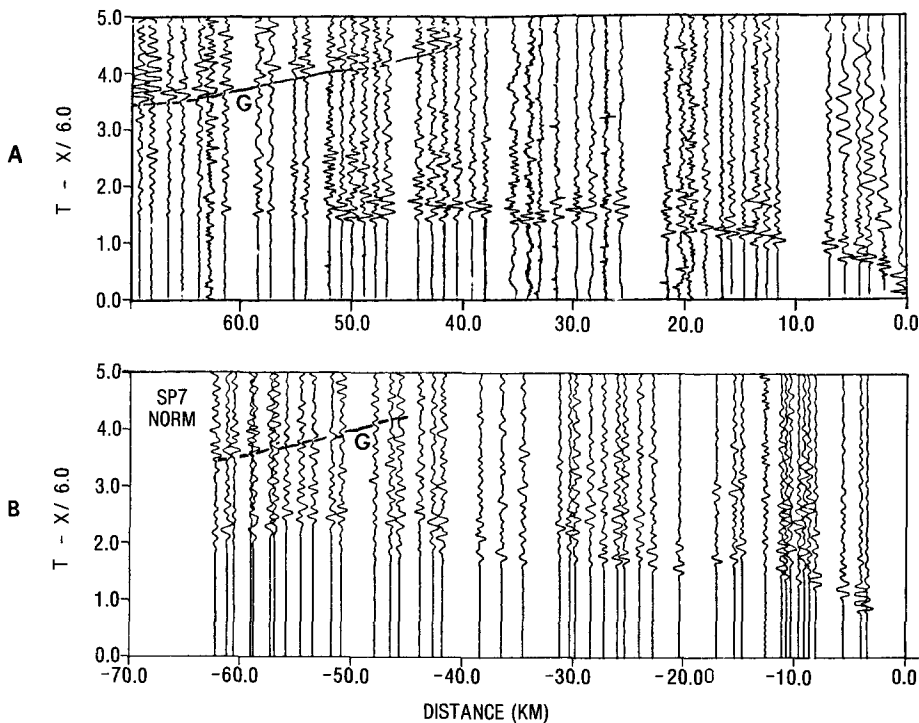


FIG. 8. Comparison of the record section for Cedar Mountain southeast (SE) in the Diablo Range (A) and the record section for shotpoint 7 (B). Cedar Mountain is 90 km north of shotpoint 7. The secondary arrivals labeled G are recorded at the same distance and at the same time. Labeling of the phases is explained in Figure 6.

4 and 7. Phases *f* and *E* (Figures 3 and 4) are interpreted as arrivals from a 3-km-thick layer with a velocity of 6.8 to 6.9 km/sec. The upper boundary of this layer lies at about 13 km depth.

The structure below 16 km has been inferred from phase *G* in the record section of the shotpoint 7; we interpret this phase as the same phase observed on the profile "Cedar Mountain southeast (SE)" in the Diablo Range (Stewart, 1968; Warren, 1978) Blümling and Prodehl (1983) have interpreted this phase as a reflection from the base of a lower crustal low-velocity zone. Figure 8 shows a comparison of the two record sections. The corresponding *G* phases can be correlated at nearly the same travel time and distance, but the apparent amplitude of the precritical reflections is smaller for the shotpoint 7 data. We therefore slightly modified the

structure of the lower crust from the interpretation of Blümling and Prodehl (1983) and included it in our model.

Figure 9 compares one-dimensional velocity-depth models for the area near Coyote Lake (this study), the Cedar Mountain SE model, and an additional model inferred from earthquake record sections compiled from the U.S. Geological Survey CALNET array (Prodehl, 1977; Blümling and Prodehl, 1983). The earthquake model is considered less reliable than the Cedar Mountain SE model due to the larger spacing of the CALNET stations as compared to the seismic refraction data. Figure 9 shows that below a depth of 14 km, all three models reach a velocity of about 6.75 km/sec, and include a low-velocity zone with a modeled velocity of about 5.3 km/sec. The lower boundary of the low-velocity zone is at about 23 km depth for the Coyote Lake and the earthquake model, and is at 25.5 km for the Cedar Mountain SE model. The presence of a pronounced low-velocity zone underlying

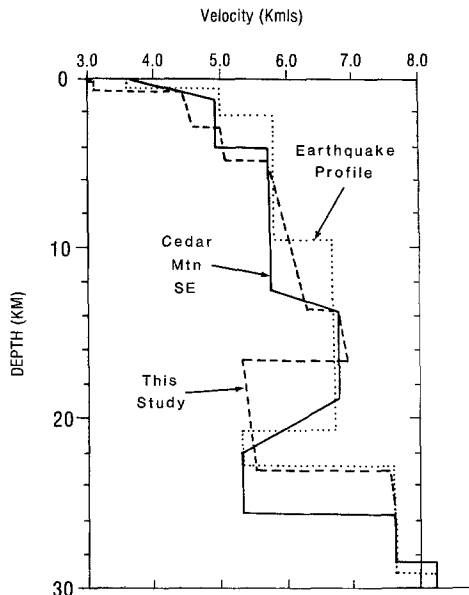


FIG. 9. Comparison between the average one-dimensional velocity-depth model developed for explosion-refraction data for the Diablo Range (solid line), for earthquake-refraction data east of the San Andreas fault (dotted line), and the Calaveras fault region (this study; dashed line).

the Diablo Range indicates a major lithologic change occurs in the lower crust. Further evidence for this lower crustal low-velocity zone is given by Murphy and Walter (1984) who present a seismic record section for the Franciscan terrain with a strong reflected phase corresponding to phase *G* of this study and Blümling and Prodehl (1983).

The travel times calculated for the velocity model of Figure 7 are within 0.05 sec of nearly all observed travel times on the profiles; the agreement is less good for shotpoint 4 between 24 and 32 km. The upper 5 km of the velocity model is sufficiently detailed to produce complex travel-time curves. It is emphasized that not every phase labeled in Figure 6 and on the travel-time curves imposed on the record sections (Figures 3 to 5) can be distinguished on each record section. The total travel-time curves of the model was imposed on the record sections to show where each phase is predicted by the model, even where the phase is unclear. For

example, phase *e* is unclear in Figure 5, although it must be present based on the evidence from shotpoints 4 and 7, and phase *d* is clear only on shotpoint 5 (Figure 5).

Modeling the observed amplitudes presented some difficulties. The synthetics match the position of the observed amplitude maxima fairly well, but the amplitude decay with distance is much more rapid for the observed data than for the synthetics; while the theoretical seismograms are multiplied only by distance, the observed seismograms have to be multiplied by distance to the 1.5 power to be visible at larger range. Even with a larger distance scaling factor for the observed data, the synthetic seismograms for shotpoints 7 and 5 NW are significantly larger than the observed seismograms (Figures 4 and 5). This is probably due to the neglect of the effects of finite *Q* and scattering in the synthetic calculation. Attenuation of seismic waves in the Calaveras fault zone has been described qualitatively in a study of earthquake data (Spudich and Angstman, 1980).

The crustal structure model of this study generally agrees with the pattern of the Bouguer gravity in this area (Figure 7). The gravity is low over the sedimentary basin near shotpoint 4 and in the southeast where the sediments thicken. The 5.1 km/sec layer corresponds to a Bouguer gravity high. A quantitative comparison of the crustal structure and the Bouguer gravity anomaly requires a consideration of three-dimensional structure and is not attempted here.

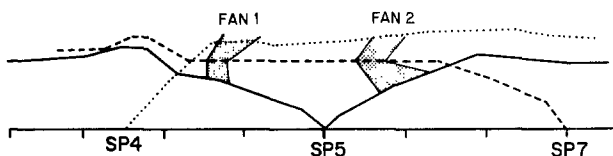


FIG. 10. Travel-time curves of the first arrivals for the three shots. The stippled areas indicate the distances from the shotpoints to the fan profiles. The reduction velocities used for the fan record sections (Figure 11) are taken from the apparent velocities of the first arrival phases in the stippled areas.

THE FAN PROFILES

In addition to the main profile, two fan profiles were recorded to investigate lateral variations in the velocity structure across the fault zone. Fan 1 was recorded between shotpoints 4 and 5, and fan 2 between shotpoints 5 and 7 (Figure 2).

The analysis method applied to the fan data is different than that applied to the main profile. To determine the appropriate reducing velocity for the fan profiles, we examined the apparent velocities of first arrivals of the main profile at the appropriate distance range (Figure 10). The distance ranges from the three shots to the two fans are shown as the stippled areas in Figure 10, and from this plot we determined, for example, a reducing velocity of 4.1 km/sec for fan 2, shotpoint 5. Using these reducing velocities, we would expect to obtain first arrivals with a constant reduced time if there were no lateral variations in velocity across the fan. Conversely, significant lateral velocity variations will appear as travel-time delays or advances.

Figure 11 shows the fan profiles plotted with the reducing velocities determined from Figure 10. The record sections for shotpoints 5 and 7 recorded by fan 1 show a narrow delayed zone directly at the fault trace. This zone, has a relative delay of 0.3 to 0.4 sec with respect to adjacent seismograms, and is less than 2 km wide perpendicular to the fault (NE-SW). We, therefore, interpret this delay as a low-velocity zone associated with the fault. For shotpoint 4, observations at fan 1 show

a significantly broader delayed zone centered at the fault trace with a maximum delay of 0.7 sec. For this shot, the delay at the fault zone is broadened by additional delays introduced by the local sedimentary basin (identified in the interpretation of the main profile and shown with a velocity of 2.6 km/sec in Figure 7).

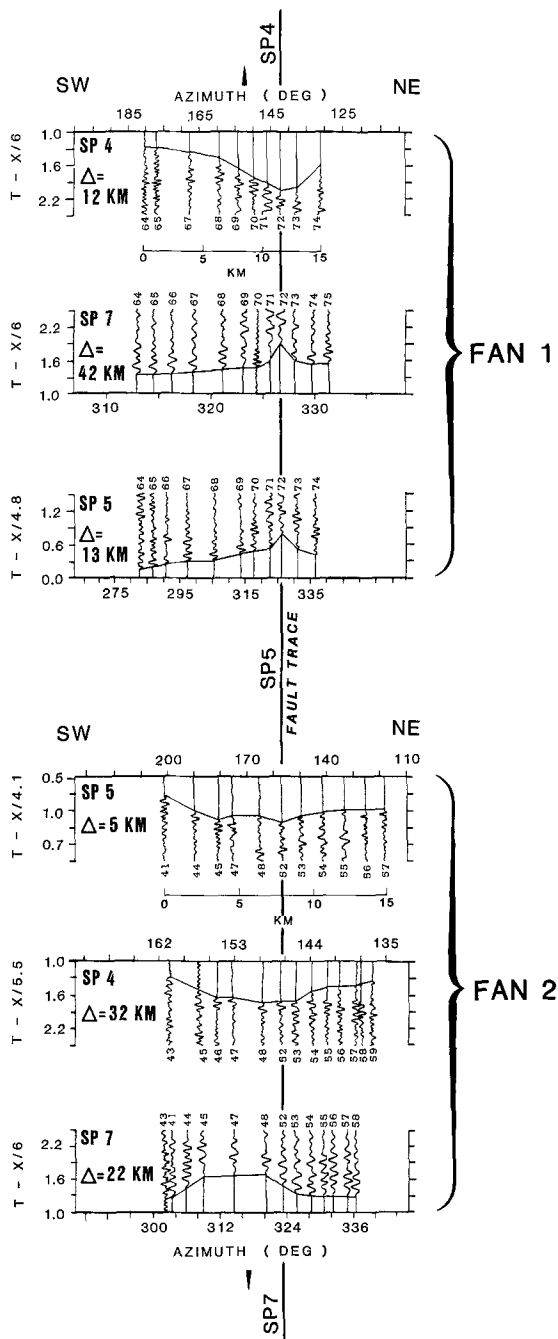


FIG. 11. Fan record sections for the two fan profiles (Figure 2) for the three shotpoints. The solid line in the middle shows the position of the surface fault trace of the Calaveras fault zone. The reduction velocities used on the various record sections are taken from Figure 10. The indicated distances (Δ) are the minimum shot-recorder distances. The approximate depth of penetration for arrivals at a given distance can be determined by examining the ray trace diagram (Figure 7).

In contrast, fan 2 shows a very broad delay zone which encompasses both the fault zone and the Santa Clara Valley. The relative delays, which range from 0.1 to 0.55 sec, are observed for all three shots. These delays do not correlate uniquely with the Santa Clara Valley, but begin east of the valley at the Calaveras fault trace. Thus, the data from fan 2 support the more unambiguous observations on fan 1 indicating a low-velocity zone about the fault zone. There are differences in the shape and magnitude of the delay zone recorded on fan 2 for the three shots; these are discussed below.

EVIDENCE FOR EN-ECHELON FAULT PLANES ON FAN 2

Aftershock hypocenters for the 6 August 1979 Coyote Lake earthquake have been determined by Reasenberg and Ellsworth (1982). The velocity model used to

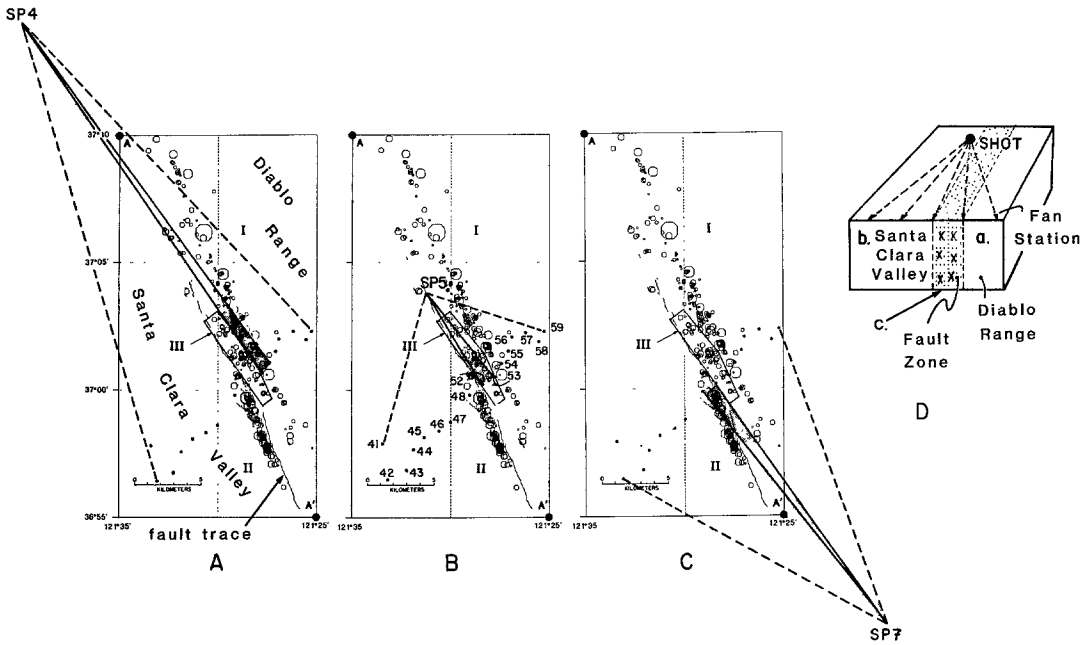


FIG. 12. Map view of the distribution of the Coyote Lake aftershocks, showing evidence of different rupture planes along the Calaveras fault zone. Seismograph locations for fan 2 are indicated by solid dots, location numbers are on panel B. Ray paths (dashed lines) to the other stations on the fan profiles are indicated for each shotpoint. Cartoon (D) explains the lateral velocity differences indicated by these observations. The shaded area is the area of travel-time delay which correlates with the rupture planes of Reasenberg and Ellsworth (1982).

determine these hypocenters was derived from an interactive least-squares velocity estimation procedure similar to that described by Crosson (1976). Since their preferred model B (including station corrections) agrees within 5 per cent at all depths with the velocity model derived in this study, we can superimpose the hypocentral locations of the aftershocks on our crustal velocity section without relocating the events. We note that Thurber (1983) obtained a similar hypocentral distribution as Reasenberg and Ellsworth (1982) using full three-dimensional methods.

Reasenberg and Ellsworth (1982) defined three regions, labeled I, II, and III (Figure 12), within the aftershock zone based on seismicity lineations. They concluded that the Calaveras fault consists principally of two nearly vertical, right-stepping en-echelon fault planes (regions I and II) and an area of diffuse seismicity

between the two planes (region III). The southwestern fault plane (region II) coincides with the fault trace while the other fault plane (region I) lies 2 km to the northeast.

Further evidence that the Calaveras fault near Coyote Lake consists of at least two subsurface fault planes comes from the seismic data of fan 2. Figure 12, A to C, shows earthquake epicenters and station locations for fan 2, and shotpoints 4, 5, and 7. As mentioned above, first arrival times on the fan profiles show time delays due to lateral changes in the near-surface velocity of the crust. The sketch in Figure 12D explains the delays observed on fan 2. While the seismograms in region "a" show normal arrival times, the first arrivals of recording stations in the Santa Clara Valley, zone "b", are delayed by 0.3 to 0.4 sec. Delays occurring east of the valley are in zone "c". If there were only one fault plane, we would expect to see this delayed zone "c" at the same station location for all three shots. Because of the en-echelon offset of the fault planes, however, the record sections for shotpoints 4 and 7 show this delay at *different* locations (Figure 11). Shotpoint 7, recorded at fan 2, shows a delay between stations 52 and 48, west of the fault trace. These station locations coincide with the fault plane of region II (Figure 12C). (We note that this delay could in part be due to the fact that shotpoint 7 is located east of the Calaveras fault.) Shotpoint 4 data shows a delay between stations 53 and 54, about 2 km northwest of the fault trace (Figure 12A), corresponding with the second fault plane, region I. Shotpoint 5 exhibits only a single delayed seismogram within a broad delay zone (station 52, Figure 11), but this correlates with the hypocenters in region III. Thus, the two principal en-echelon fault planes and the smaller intermediate zone of seismicity defined by Reasenber and Ellsworth (1982) are distinguishable on the basis of travel-time delays on the fan 2 profiles.

SEISMICITY AND CRUSTAL STRUCTURE

To determine which portions of the crust are seismically active, we have superimposed the hypocentral locations presented by Reasenber and Ellsworth (1982) on the velocity structure modeled in this study. Most of the seismicity is located in the layer that grades in velocity from 5.7 to 6.3 km/sec. However, we note that in regions I and III, nearly all shallow earthquakes (<5 km) are located in the high-velocity body (5.0 to 5.2 km/sec), while very few earthquakes occur in the surrounding sediments. The high-velocity body presumably has a higher shear strength than the surrounding formation and it may therefore act as an asperity along the fault zone.

The correlation of seismicity with the higher velocity is less clear in region II. However, region II lies 2 to 3 km southwest of our main profile line and, thus, this may be the effect of projecting events onto the plane of the refraction profile cross section. Thurber (1983) has also determined a high-velocity body at a similar depth which crosses the fault zone in this region and extends to the southwest. If the high-velocity body were extended 5 km southwest of region II, the earthquakes would indeed be confined to this body or the layer below.

DISCUSSION AND CONCLUSIONS

This investigation has addressed two main topics, the crustal velocity structure along and across the Calaveras fault, and the relationship between fault structure and seismicity patterns. We discuss these topics in turn.

The main profile along the Calaveras fault is unusual in that it was largely recorded along what we demonstrate to be a vertical seismic low-velocity zone. We

therefore expect that the first arrivals at receivers within the fault zone will travel through the surrounding higher velocity media. In this case, we may ask, what is the physical interpretation of the two-dimensional velocity model of Figure 7? The fan profile data show that the seismic low-velocity zone along the fault is 1 to 2 km wide. This indicates that for a shotpoint-receiver pair located along the fault, the first arrivals will refract 1 to 2 km out of the plane. We therefore interpret the model of Figure 7 to correspond to the higher velocities encountered within the crust along a 4-km wide strip connecting the shot points. The velocities within the fault zone itself are lower than those of Figure 7.

The crustal velocity structure (Figure 7) can be compared with the surface geology and velocities derived from previous seismic-refraction studies in order to determine lithology. The lithologies of the near-surface layers are known from geologic mapping (Figure 2). These layers consist of a range of rock types with seismic velocities between 2.75 and 3.2 km/sec. The major new results for the near-surface structure are the resolution of the basin near shotpoint 4 and the determination of the depth of the alluvial fill in the southern Santa Clara Valley.

A prominent feature of the crustal structure is the velocity discontinuity at a depth of about 4.5 km. Where the 5.1 km/sec layer does not occur, this discontinuity is interpreted as the contact between the Great Valley Sequence and the underlying Franciscan assemblage. There are several reasons for this interpretation. First, the Great Valley Sequence occurs at the surface along much of this profile and is known to overlie the Franciscan assemblage in the neighboring Diablo Range. Second, the seismic velocity of the 4.2 to 4.7 km/sec layer is similar to that determined for the Great Valley Sequence elsewhere (Mooney and Walter, 1981), and the velocity of the underlying layer (5.7 to 6.3 km/sec) agrees with the velocities of the Franciscan assemblage in the Diablo Range (Walter and Mooney, 1982). We therefore conclude that the Great Valley Sequence has a regional thickness of 3 to 4 km along the seismic profile, except beneath shotpoint 5 where the higher velocity body (5.0 to 5.2 km/sec) occurs. We interpret the high-velocity body to consist of volcanic rocks on the basis of the surface geologic exposure and its seismic velocity which is intermediate between that of the Great Valley Sequence and the Franciscan assemblage.

The velocity structure below 10 km has not been well determined by this relatively short refraction profile. However, since we have observed a phase which correlates with the observations of Blümling and Prodehl (1983) in the neighboring Diablo Range, we have adopted a lower crustal model similar to theirs (Figure 9). The 6.8 to 6.9 km/sec layer is interpreted as mafic igneous rocks beneath the Franciscan assemblage and may represent oceanic crust (Walter and Mooney, 1982). The underlying low velocity layer (5.3 to 5.5 km/sec) almost certainly would have to consist of sedimentary rocks. If our lithologic interpretations of these layers is correct, it suggests that large scale thrusting has occurred during the accretion of the Diablo Range, placing the Franciscan assemblage and associated igneous oceanic rocks over lower velocity rocks. The improved resolution of the lower crustal velocity structure of central California is the subject of continuing investigation.

Comparing the local velocity structure of the Calaveras fault zone with the hypocenters of the aftershocks of the Coyote Lake earthquake (Reasenber and Ellsworth, 1982) we conclude that the earthquakes are restricted to the inferred volcanic body and the Franciscan assemblage, and do not occur within the Great Valley Sequence or overlying sedimentary rocks. Shallow earthquakes correlate with the volcanic body and are concentrated at its edge (Figure 13, b and c). This body therefore appears to act as an asperity on the fault zone.

The shape and structure of the Calaveras fault zone has been inferred from the fan profiles. Travel-time delays at fan 1 show a vertical near-surface low-velocity zone, 1 to 2 km wide, which is directly related to the fault, as postulated by Mayer-

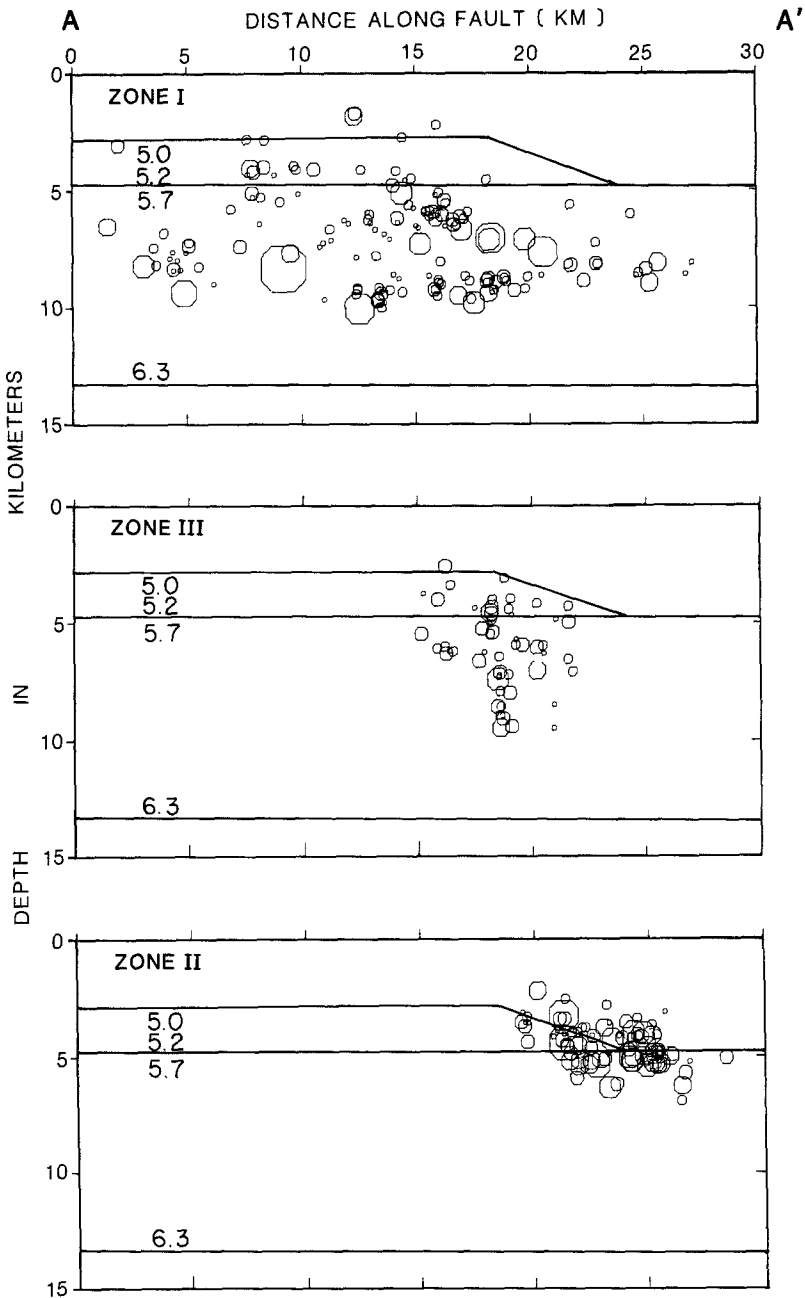


FIG. 13. Hypocentral distribution of the Coyote Lake earthquake and its aftershocks (Reasenber and Ellsworth, 1982) in comparison to the crustal structure calculated for the seismic-refraction data. Zones I, II, and III, and cross-section line A-A' are defined in Figure 12.

Rosa (1973). At fan 2, the delays due to this low-velocity zone merge with the broader delay produced by the low-velocity alluvium of the Santa Clara Valley (Mooney and Luetgert, 1982). When examined in detail, the fan 2 data provide

further evidence for the two en-echelon fault planes defined by seismicity lineaments (Reasenber and Ellworth, 1982).

ACKNOWLEDGMENTS

We thank the U.S. Geological Survey field staff for their diligent efforts in collecting the seismic refraction data used in the study: E. E. Criley, R. P. Meyer, Jr., V. D. Sutton, L. R. Hoffman, J. N. Roloff, S. S. Gallanthine, G. A. Molina, J. Van Schaak, and W. M. Kohler. Comments on the manuscript by M. C. Andrews, G. S. Fuis, J. H. Luetgert, D. H. Oppenheimer, B. M. Page, P. A. Reasenber, and P. A. Spudich are appreciated. Suggestions by an anonymous reviewer substantially improved the manuscript.

REFERENCES

- Bakun, W. H. (1980). Seismic activity on the southern Calaveras fault in central California, *Bull. Seism. Soc. Am.* **70**, 1181–1197.
- Blümling, P. and C. Prodehl (1983). Crustal structure beneath the eastern part of the Coast Ranges (Diablo Range) of central California from exposure-seismic and near-earthquake data, *Physics Earth Planet Interiors* **31**, 313–326.
- Červený, V., I. A. Molotov, and I. Pšenčík (1977). *Ray Method in Seismology*, University of Karlova, Prague, Czechoslovakia, 214 pp.
- Crosson, R. S. (1976). Crustal structure modeling of earthquake data. 1. Simultaneous least squares estimation of hypocenter and velocity parameters, *J. Geophys. Res.* **81**, 3036–3046.
- Herd, D. G. (1979). Neotectonic framework of central coastal California and its implications to microzonation of the San Francisco Bay region, *U. S. Geol. Surv. Circular* **807**, 3–12.
- Herd, D. C. and D. S. McCulloch (1983). Map of the principal recently active faults in the San Francisco Bay region and surrounding California Coast Ranges, *U.S. Geol. Surv. Misc. Field Study Map*.
- Lee, W. H. K., D. G. Herd, V. Cagnetti, W. H. Bakun, and A. Rapport (1979). A preliminary study of the Coyote Lake earthquake of August 6, 1979, and its major aftershocks, *U.S. Geol. Surv., Open-File Rept. 79-1621*, 43 pp.
- Mayer-Rosa, D. (1973). Travel-time anomalies and distribution of earthquakes along the Calaveras fault zone, California, *Bull. Seism. Soc. Am.* **63**, 713–729.
- McMechan, G. A. and W. D. Mooney (1980). Asymptotic ray theory and synthetic seismograms for laterally varying structures: theory and application to the Imperial Valley, California, *Bull. Seism. Soc. Am.* **70**, 2021–2035.
- Mooney, W. D. and A. W. Walter (1980). Seismic refraction studies in the Coast ranges, central California (abstract), *EOS* **62**, 328.
- Mooney, W. D. and J. H. Luetgert (1982). A seismic refraction study of the Santa Clara Valley and the southern Santa Cruz Mountains, west-central California, *Bull. Seism. Soc. Am.* **72**, 901–909.
- Murphy, J. M. and A. W. Walter (1984). Data report for a seismic-refraction investigation: Morrow Bay to the Sierra Nevada, California, *U.S. Geol. Surv. Open-File Rept. 84-642*, 37 pp., 12 plates.
- Page, B. M. (1982a). Modes of Quaternary tectonic movement in the San Francisco Bay region, California, *Calif. Div. Mines Geol., Spec. Publ.* **62**, 1–10.
- Page, B. M. (1982b). The Calaveras fault zone of California—An active plate boundary element, *Calif. Div. Mines Geol., Spec. Publ.* **62**, 175–184.
- Prodehl, C. (1977). Record sections for selected local earthquakes recorded by the central California microearthquake network, *U.S. Geol. Surv., Open-File Rept. 77-37*, 310 pp.
- Reasenber, P. and W. L. Ellsworth (1982). Aftershocks of the Coyote Lake, California earthquake of August 6, 1979: a detailed study, *J. Geophys. Res.* **87**, 10637–10655.
- Spudich, P. A. and B. G. Angstman (1980). Lateral variations in velocity and Q structure in the region of the 1979 Coyote Lake, California earthquake (abstract), *Earthquake Notes* **5**, 64.
- Stewart, S. W. (1968). Preliminary comparison of seismic traveltime and inferred crustal structure adjacent to the San Andreas fault in the Diablo and Gabilan Ranges of central California, in Geological Problems of San Andreas Fault System Conf. Proc., W. R. Dickinson, and A. Grantz, Editors, *Stanford Univ. Publ. Geol. Sci.* **11**, 218–230.
- Thurber, C. H. (1983). Earthquake locations and three-dimensional crustal structure in the Coyote Lake Area, central California, *J. Geophys. Res.* **88**, 8226–8236.

- Walter, A. W. and W. D. Mooney (1982). Crustal structure of the Diablo and Gabilan Ranges, Central California: a reinterpretation of existing data, *Bull. Seism. Soc. Am.* **72**, 1567-1590.
- Warren, D. H. (1978). Record sections of two seismic refraction profiles in the Gabilan and Diablo Ranges, California, *U.S. Geol. Surv., Open-File Rept.* 78-340, 12 pp.

U.S. GEOLOGICAL SURVEY
345 MIDDLEFIELD ROAD, MS 77
MENLO PARK, CALIFORNIA 94025

Manuscript received 15 March 1984